Uncertainty Quantification of Demand Response Datasets using Peridynamics

Andrew Rosener, Katelyn Koiner and Prakash Ranganathan
Department of Electrical Engineering
University of North Dakota, Grand Forks, ND 58202

***Abstract*— This paper investigates curve-fitting methods to explore uncertainty quantification approaches for demand fluctuations in a power grid. Specifically, we use data sets from the *Pennsylvania–New Jersey–Maryland* (PJM) Interconnection, where we employ two stages of fitting. In stage one, a trigonometric based fit for historical data sets is carried out. In stage two, load forecasting for day-ahead market is developed using peridynamics under uncertainty conditions. The preliminary results from this two-stage approach were promising for resource planning and energy management tasks. This work will allow system operators to capture both stable and non-stable operation early enough to perform planning tasks related to the microgrid.**

Keywords: uncertainty, peridynamics, curve-fitting, load modeling

I. Introduction

In recent years, microgrid technology has begun to advance from strictly theoretical to real-world application, as the number of microgrid projects continue to grow across the globe [1]. A *microgrid* is a localized grouping of electric supply sources and loads that normally operates with, and is connected to, the traditional centralized grid but can also disconnect and function autonomously as physical and economic conditions dictate.

The integration of microgrids into our power networks has the potential to facilitate the modernization of energy grids, and assist our transition to more efficient, secure, and reliable energy distribution systems. In this paper, we investigate data driven control using peridynamics and PJM data sets, as outlined by the flow chart in Figure 1. First, we fit a trigonometric function to the PJM data using a Fourier series algorithm to obtain $D(t)$ in order to represent PJM's (discrete, hourly) data as a continuous function of time. We also use the PJM data to calculate the standard deviation, σ, and mean, μ, for a specified range. We can then use μ and σ to calculate the *level of uncertainty* (LOU) in the demand. Equipped with the LOU in the demand and the trigonometric fit of the original data, we can create a new function, $\hat{D}(t)$, that simulates uncertainty in real-world demand profiles. Using supply information and $\hat{D}(t)$, we are able to model the pairwise force function, $f(t)$, that is used in peridynamic modeling.

The remaining sections of the paper are divided as follows: section 2: Peridynamic Theory, section 3: Load Fitting, section 4: Uncertainty Quantification, section 5: Load Modeling, and section 6: Conclusion.

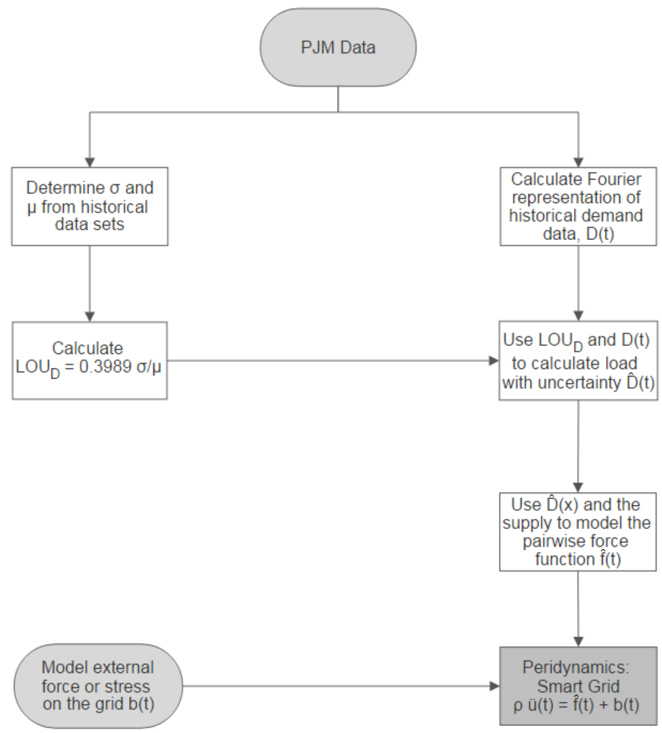

Fig. 1. Flow chart displaying the structure of the microgrid modeling process using peridynamics.

II. Peridynamic Theory

Advancing fields, particularly those relating to failure propagation modeling in material science heavily rely on partial differential equations which are not sufficient to describe fractures. These methods also require one to know the location of the fractures ahead of time [2]. This is especially limiting, when considering spontaneous formation of discontinuities, when one likely does not know the location of the discontinuities in advance.

The field of peridynamics allows particles to interact at a distance, eliminating the assumption of particle interaction being strictly due to contact forces.

Since the integral form of peridynamic equations remain undaunted by discontinuities, it is not necessary to know their location prior to application of the model. Moreover, this lends the unique ability to predict the location at which fractures will occur within the material. This powerful ability

Variable	Definition
$\alpha, \beta, \gamma, \delta, \epsilon$	Fourier coefficients
b	External force
$\mathcal{B}$	A closed, bounded body
D	PJM fitted data
$\hat{D}$	PJM fitted data with uncertainty
e	Bond elongation
f	Pairwise force function
$\hat{f}$	External force density field
I, J, K, L	Trigonometric fit parameters
$\mathcal{L}$	Standardized loss function
μ	Mean
ρ	Mass density
σ	Standard deviation
S	Supply
t	Time
u, u'	Displacement of x, x'
V	Volume
x, x'	Particle

can be significantly useful in smart grid applications. We show how peridynamics can assist in the quantification of uncertainties related to demand and supply fluctuations that can reduce outages and cascading failures in the power grid.

A. The Peridynamic Equation of Motion

To apply peridynamics to the smart grid domain, a basic understanding of the core equations related to this topic is warranted. The following derivation addresses how materials behave and interact internally in the presence of external forces, as well as how the material reacts as a whole.

Let $\mathcal{B}$ be a closed, bounded body with mass density $\rho(\boldsymbol{x})$, $\boldsymbol{u}(\boldsymbol{x}, t)$ be the position of a particle $\boldsymbol{x}$ at time t in the body, $\boldsymbol{b}(\boldsymbol{x}, t)$ be the external body force density field, and $\hat{\boldsymbol{f}}(\boldsymbol{x}, t)$ be the internal force density on x at time t. Now assume there is an asymmetric vector-valued function $\boldsymbol{f}$ such that

$$\hat{\boldsymbol{f}}(\boldsymbol{x}, t) = \int_{\mathcal{B}} \boldsymbol{f}(\boldsymbol{x'}, \boldsymbol{x}, t)\ dV'. \qquad \forall\ \boldsymbol{x} \in \mathcal{B}, t \geq 0.$$

Then, from Newton's second law of motion, the peridynamic equation of motion is given by,

$$\rho(\boldsymbol{x})\ddot{\boldsymbol{u}}(\boldsymbol{x}, t) = \int_{\mathcal{B}} \boldsymbol{f}(\boldsymbol{x'}, \boldsymbol{x}, t)\ dV' + \boldsymbol{b}(\boldsymbol{x}, t). \qquad (1)$$

This result is the peridynamic equation of motion proposed in [3], and is used to describe the motion of the material body in question at any point in time. The first term on the RHS of equation 1 will incorporate actual demand datasets and a supply model. The second term on the RHS of equation 1 will incorporate a model for the external force on the grid, such as a random exponential increase in the load.

B. The Pairwise Force Function

The function $\boldsymbol{f}$ appearing within the integrand of equation 1 is such an important part of the result that the phrase *pairwise force function* was created to describe this function [3]. The pairwise force function plays an integral role in the

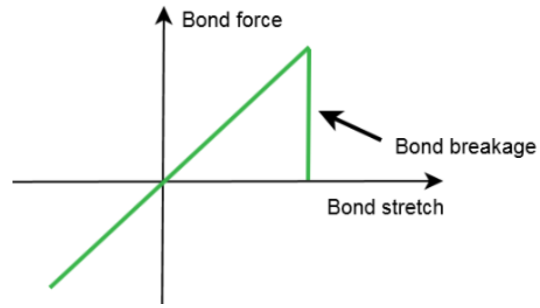

Fig. 2. The pairwise force function seen in equation 1 the peridynamic equation of motion.

ability of peridynamics to consider the individual interactions of discrete points in the model, as $\boldsymbol{f}(\boldsymbol{x}, \boldsymbol{x'}, t)$ is analogous to the force vector $\boldsymbol{x'}$ exerts on $\boldsymbol{x}$. This can be visualized by graphing the force function versus bond elongation. The bond in question is referring to a bond between the point $\boldsymbol{x}$ and some point $\boldsymbol{x'}$. The elongation, e, is described by the difference between the final bond length and the initial bond length, is given by $e = |(\boldsymbol{x'} + \boldsymbol{u'}) - (\boldsymbol{x} + \boldsymbol{u})| - |\boldsymbol{x'} - \boldsymbol{x}|$. The graph of $\boldsymbol{f}$ as a function of e, shown in Figure 2, displays how the force changes due to deformation and most notably highlights the point at which the force instantaneously drops to zero, representing the bonds within the material breaking.

If we construct a pairwise force function that interprets force as stress experienced by a subset of generators within a microgrid accommodating failure conditions, this function can model the time at which generators can fail. The application of peridynamics to smart grid concepts has great potential in solving real-time planning issues related to microgrid projects. Additionally, implementation of load forecasting has the potential to yield an improved warning method to reduce outage and reaction times that can prevent cascading grid failures.

III. Load Fitting

In order to apply peridynamic theory to a load model, a mathematical function must be found which accurately represents the load profile of historical data sets. Our approach to this involves curve fitting methods using real world data from the PJM database which summarizes the MW-hour net energy for load consumed by the territories serviced by PJM

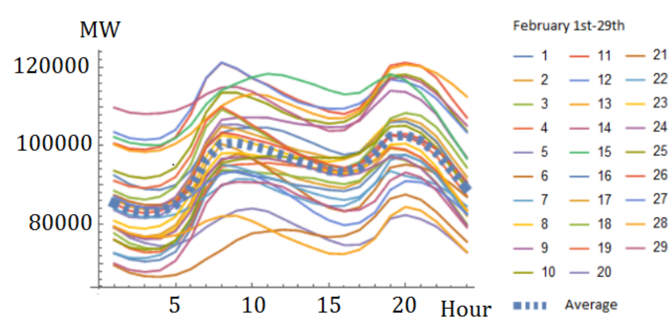

Fig. 3. February 2016 PJM RTO average load in MW, displaying every day of the month and their average, plotted over 24 hours.

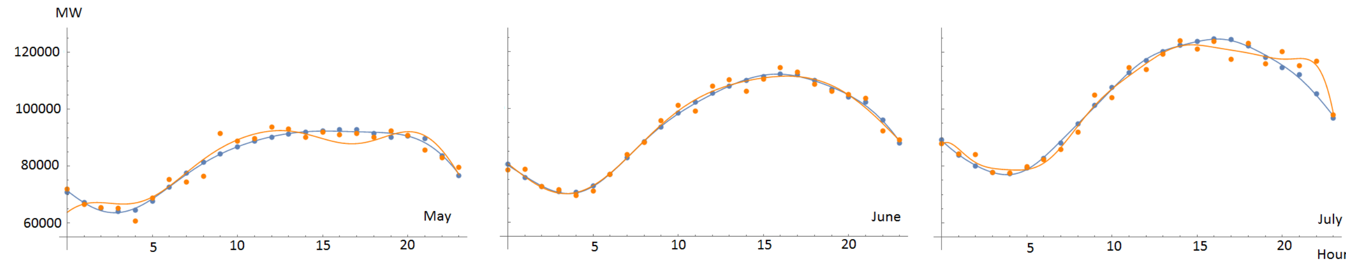

Fig. 4. Trigonometric fits for PJM RTO data for select momths over a 5 year weekday average, plotted over a 24-hour period. Blue curve: $D(t)$, load function without uncertainty, orange curve: $\hat{D}(t)$, load function with uncertainty.

Month		Trigonometric Demand Functions
May	$D(t)$	$53647.7 + 14535.9\mathbf{C}[0.0558726t] + 14535.9\mathbf{C}[0.0558726t] + 6922.75\mathbf{C}[0.111745t] + 6922.75\mathbf{C}[0.111745t] - 12612.5\mathbf{C}[0.167618t] - 12612.5\mathbf{C}[0.167618t] - 3097.13\mathbf{S}[0.251079t] - 3097.13\mathbf{S}[0.251858t] - 2308.38\mathbf{S}[0.502158t] - 2308.38\mathbf{S}[0.503715t] - 510.797\mathbf{S}[0.753237t] - 510.797\mathbf{S}[0.755573t]$
	$\hat{D}(t)$	$52641.5 + 4494.37\mathbf{C}[0.293777t] + 5289.58\mathbf{C}[0.587553t] + 1278.82\mathbf{C}[0.88133t] - 41540.5\mathbf{S}[0.0172519t] - 41540.5\mathbf{S}[0.017267t] - 41540.5\mathbf{S}[0.0173036t] - 53167.7\mathbf{S}[0.0345039t] - 53167.7\mathbf{S}[0.034534t] - 53167.7\mathbf{S}[0.0346073t] + 5167.42\mathbf{S}[0.0517558t] + 5167.42\mathbf{S}[0.051801t] + 5167.42\mathbf{S}[0.0519109t] + 54896.5\mathbf{S}[0.0690077t] + 54896.5\mathbf{S}[0.069068t] + 54896.5\mathbf{S}[0.0692145t]$
June	$D(t)$	$100526 - 7372.41\mathbf{C}[0.193696t] - 7372.41\mathbf{C}[0.194377t] - 7372.41\mathbf{C}[0.269632t] - 701.178\mathbf{C}[0.387392t] - 701.178\mathbf{C}[0.388755t] - 701.178\mathbf{C}[0.539265t] + 1258.68\mathbf{C}[0.581088t] + 1258.68\mathbf{C}[0.583132t] + 1258.68\mathbf{C}[0.808897t] - 39089.6\mathbf{S}[0.0491453t] - 4408.73\mathbf{S}[0.0982906t] + 39890.4\mathbf{S}[0.147436t] - 37347.2\mathbf{S}[0.196581t]$
	$\hat{D}(t)$	$63439.6 + 17210.8\mathbf{C}[0.0934771t] + 11270\mathbf{S}[0.0860162t] + 11270\mathbf{S}[0.0860518t] + 11270\mathbf{S}[0.112666t] + 11270\mathbf{S}[0.140454t] - 5957.44\mathbf{S}[0.172032t] - 5957.44\mathbf{S}[0.172104t] - 5957.44\mathbf{S}[0.225332t] - 147.312\mathbf{S}[0.258049t] - 147.312\mathbf{S}[0.258155t] - 5957.44\mathbf{S}[0.280908t] - 147.312\mathbf{S}[0.337998t] - 2516.41\mathbf{S}[0.344065t] - 2516.41\mathbf{S}[0.344207t] - 147.312\mathbf{S}[0.421362t] - 2516.41\mathbf{S}[0.450664t] - 2516.41\mathbf{S}[0.561816t]$
July	$D(t)$	$91128.1 - 1651.28\mathbf{C}[0.440453t] - 28.4958\mathbf{C}[0.880906t] - 410.607\mathbf{C}[1.32136t] + 5211.31\mathbf{S}[0.131961t] + 5211.31\mathbf{S}[0.131961t] + 5211.31\mathbf{S}[0.131961t] + 5211.31\mathbf{S}[0.131962t] - 5122.28\mathbf{S}[0.263922t] - 5122.28\mathbf{S}[0.263922t] - 5122.28\mathbf{S}[0.263922t] - 5122.28\mathbf{S}[0.263924t] - 1401.92\mathbf{S}[0.395882t] - 1401.92\mathbf{S}[0.395882t] - 1401.92\mathbf{S}[0.395882t] - 1401.92\mathbf{S}[0.395885t] - 380.268\mathbf{S}[0.527843t] - 380.268\mathbf{S}[0.527843t] - 380.268\mathbf{S}[0.527843t] - 380.268\mathbf{S}[0.527847t]$
	$\hat{D}(t)$	$82924.1 - 227064\mathbf{C}[0.283458t] + 315966\mathbf{C}[0.566916t] - 84304.8\mathbf{C}[0.850373t] - 21744.1\mathbf{S}[0.173987t] - 21744.1\mathbf{S}[0.214575t] - 21744.1\mathbf{S}[0.234246t] - 21744.1\mathbf{S}[0.253386t] + 115271\mathbf{S}[0.347975t] + 115271\mathbf{S}[0.42915t] + 115271\mathbf{S}[0.468492t] + 115271\mathbf{S}[0.506773t] - 80974.6\mathbf{S}[0.521962t] - 80974.6\mathbf{S}[0.643725t] + 10115.5\mathbf{S}[0.695949t] - 80974.6\mathbf{S}[0.702738t] - 80974.6\mathbf{S}[0.760159t] + 10115.5\mathbf{S}[0.8583t] + 10115.5\mathbf{S}[0.936984t] + 10115.5\mathbf{S}[1.01355t]$

Table 1. Trigonometric functions for weekdays averaged over 2012-2016 without uncertainty, $D(t)$, and with uncertainty, $\hat{D}(t)$. The notation C[t] and S[t] has been used in replace of Cos[t] and Sin[t], respectively.

RTO. Using Wolfram Mathematica, these reports were imported and formatted for use in a user-defined function that allows custom date ranges to be easily visualized with simple parameter definitions. These ranges result in a plot of daily load as a function of time, as seen in Figure 3. As an alternative to using each day in the chosen range, options are available to only consider weekdays or weekends. Ranges are not restricted to any particular set of days, and can be chosen to be values between 1 and 365. To allow the comparison of specified data ranges across multiple years, another function was defined to construct graphs of multiple year averages for desired ranges. In the PJM RTO data sets, some hours were missing a recorded load. To address this, we took the average of the hour before and after the missing entry, and this value was used in place of the missing entry.

We have implemented a trigonometric fit algorithm using Mathematica's function NonlinearModelFit. The model used to fit the demand is given by the function D(t),

$$D(t) = \alpha_0 + \sum_{i=1}^{I}\sum_{j=1}^{J} \beta_i sin(i\gamma_j t) + \sum_{k=1}^{K}\sum_{l=1}^{L} \delta_k cos(k\epsilon_l t) \quad (2)$$

which is in the form of a Fourier series [4]. The variables I, J, K, and L can be set to choose the number of sine and cosine terms in the fit model, and Mathematica uses these parameters to find the coefficients that best fit the data [5], [6].

Figure 4 shows the trigonometric fits generated for a 5 year weekday average for the months May, June, and July. The blue curve represents the fit of the PJM load data D(t), while the orange curve represents the fit of the load data with uncertainty $\hat{D}(t)$. Table 1 lists the previously mentioned trigonometric functions for those months. The method to determine the function $\hat{D}(t)$ from $D(t)$ is discussed in detail in the following section.

IV. Uncertainty Quantification

We incorporate uncertainty into this model in two different ways. The first is by considering the level of uncertainty in the demand, and the second is by incorporating a random exponential increase in the demand to simulate an event such as severe weather that might cause a random surge in the demand.

A. *Level of Uncertainty in the Demand*

We have chosen to model the uncertainty in the demand using the the *level of uncertainty* presented in [7]. The level of uncertainty in the demand (LOU_D) is described by the following equation,

$$LOU_D = \frac{\sigma}{\mu}\mathcal{L}(0) \tag{3}$$

where σ and μ are the standard deviation and expected value of the historical data and $\mathcal{L}$(x) is the standardized loss function.

PJM metered load data was fit with a trigonometric function using the process outlined in section III, and uncertainty in the demand was calculated using equation 5. The data points for demand with uncertainty factor are generated with a 95% chance of being inside the LOU uncertainty curves to represent a fluctuating load with uncertainty.

The LOU_D is then incorporated into the demand profile by evaluating equation 3 using the calculated value of σ and μ from the historical average, as well as the value for $\mathcal{L}(0)$, yielding a constant value dependent on the historical load data for a chosen set of dates. The upper and lower bounds of load uncertainty can then be found from the product of this constant and the function from the fitted data set D(t). These bounds represent the range in which approximately 95% of the historical data falls, and can be seen in Figure 5 represented by the red dashed lines.

The LOU_D incorporated in the modeled load profile simulates the uncertainty present in real world load profiles by taking the product at time t of D(t) and a random variate generated from a normal distribution with a mean value given by D(t) and standard deviation $\frac{1}{2}LOU_D$. This process is outlined in Algorithm 1.

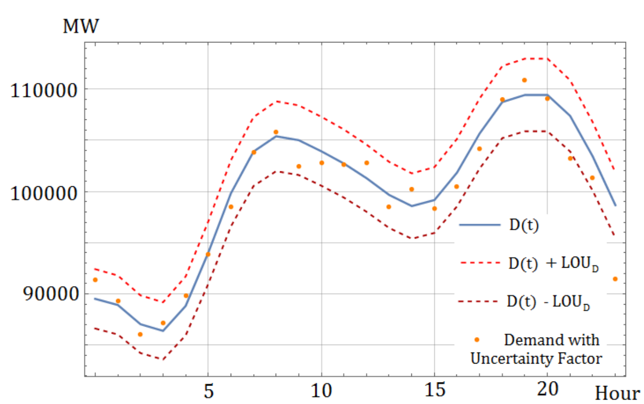

Fig. 5. Plot of D(t) and the DUF values obtained from D(t) using the process outlined in algorithm 1.

Algorithm 1: Calculate Demand with Uncertainty Factor

Input: PJM fitted data: D(t)
Determine σ and μ from historical data
Calculate LOU_D
for *t* in *D(t)*
  Evaluate D(t)
  Obtain random variate for uncertainty:
   $RV =$ RandomVariate[
     NormalDistribution[0, $\frac{1}{2}LOU_D$]]
  $DUF = D(t) * RV$
  Store values
end while
Output: PJM data with uncertainty factor (DUF)

The resulting model is able to then generate load values with a simulated uncertainty, as can be seen represented by the orange data points in Figure 5. These data points can be fitted using the same process as outlined in section III. The best fit function for the demand values with the uncertainty factor is denoted $\hat{D}(t)$, which was mentioned earlier in reference to Figure 4 and Table 1.

B. *Random Exponential Increase*

In the peridynamic equation of motion, the function **b**(t) represents the external forces on the body. In our simulation, we have chosen to model **b**(t) as some external force on the generator, such as a random spike in the demand from some external cause, e.g. severe weather. For this reason we have chosen to model this as an exponential increase in the demand, which can be seen in Figure 6 represented by the function graphed in purple. For comparison, we have also shown the original PJM fitted load data graphed in blue. The random exponential increase is modeled using Algorithm 2.

The random exponential increase we have chosen for the b(t) term is simply one of many potential uncertainties, and

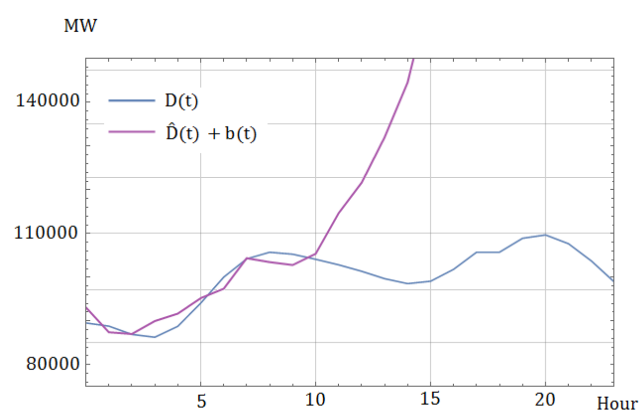

Fig. 6. Blue: the PJM fitted load data, purple: the load with uncertainty factor undergoing a random exponential increase at hour 10.

Algorithm 2: Demand Fluctuations Modeled as Exponential Function

Input: Fitted load data with uncertainty factor: $\hat{D}$(t)
Initialization
while t $<$ 24
  if *Randomness Condition* $=$ *True*
    b(t) = $e^x * \hat{D}(t)$
    Increment x
  else
    $\hat{D}(t) = \hat{D}(t)$
end while
Output: Graph $\hat{D}$(t) + b(t)

serves as an example of how to include them in our load model. Alternative uncertainties can be included to improve simulation by representing b(t) as a linear combination of additional b(t) terms, i.e. $b(t) = b_1(t) + b_2(t) + ... + b_n(t)$. Each $b_n(t)$ can be included in the model by using an algorithm similar to Algorithm 2, which is then used in the simulation by the methods discussed in section V: Load Modeling.

V. Load Modeling

The complete modeling process of demand data with external force function is said to include the following representation: $\hat{D}(t) + b(t)$, and the supply can be modeled based on the level of demand given by this representation.

A. Modeling the Supply

The supply model assumes a limited supply, determined from the sum of all hourly load values in a 24 hour period given by D(t), which depletes every hour according to the demand at time *t*. The supply model also uses a spinning reserve, or a backup generator, represented by a percentage of the overall daily load. By setting a threshold for when the load reaches some fraction of the remaining supply, the backup generator can be signaled to redistribute the reserve power to the main grid in order to avoid failure. A second threshold value can also be set which simulates generator failure when the load reaches this threshold, representing load values exceeding the set threshold of both primary and reserve supply.

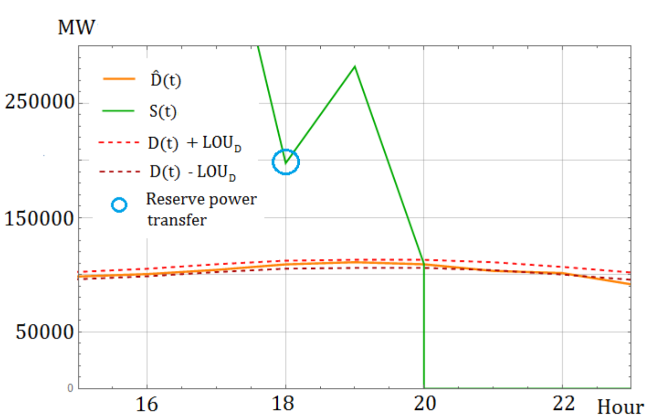

Fig. 7. Pairwise force function modeling supply and load.

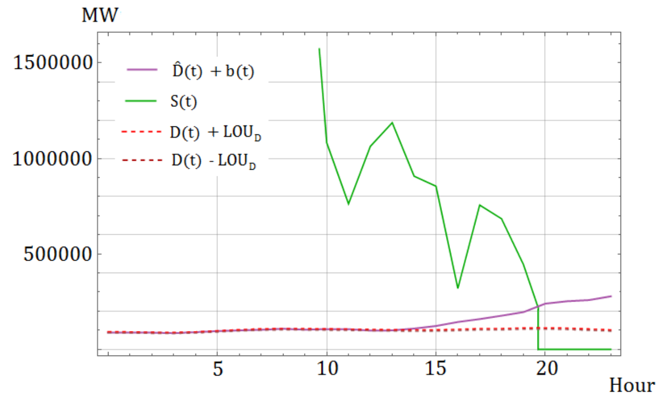

Fig. 8. Modeling the supply fluctuations as a random exponential function.

B. Failure Simulation

When supply thresholds are exceeded, the model must simulate a failure. Although our model currently uses only one failure condition, additional conditions can be included within the logic of the if statement outlined in Algorithm 3 in order to simulate other failures one may wish to model.

A failure simulation due to demand levels exceeding a finite supply and only able to be refilled daily is illustrated in Figure 7, and the algorithm used to simulate the failure is presented in Algorithm 3. Note the similarities between the pairwise force function and models at the failure points.

Upon failure, the load that was originally supplied by the failing generator must be redistributed. This load redistribution can take place in a number of ways, each of which would stress affected generators. Some examples of the scenarios that could be considered are: load redistribution to single or multiple generators and the dependence of generator strain on redistribution rate, if excessive redistribution rate can lead to cascading failures or if other factors play a larger role.

The behavior in Figure 7 indicates the transfer of reserve power to a subset of generators nearing a failure condition. For the purposes of our paper, nearing a failure condition is defined to be the load reaching a value that is equal to or less than 20% of the remaining supply. This transfer prevents

Algorithm 3: Contingency Failure Case Simulation

Input: $D(t)$
Call algorithm 1
Call algorithm 2
while t $<$ *24*
  if $\hat{D}(t) + b(t) \leq$ *80% of remaining supply*
    Subtract $\hat{D}(t) + b(t)$ from remaining supply
  else
  Remaining supply = remaining supply + reserve
    if $\hat{D}(t) + b(t) \leq$ *Remaining supply*
      Subtract $\hat{D}(t) + b(t)$ from remaining supply
    else
      Simulate Failure
end while
Output: Failure simulation graph

failure and sustains the demand for an additional 2 hours before reaching the failure condition. Note the similarities with Figure 2.

The differences in Figures 7 and 8 is that Figure 7 show no fluctuations with supply, and Figure 8 shows a sudden fluctuation within generations. This indicates the resources are exhausted more quickly in Figure 8 than Figure 7.

VI. Conclusion

The paper investigated curve-fitting methods for microgrid datasets for PJM corporation. Our preliminary results provide promising insight on peridynamic applications to smart grids. We have shown how demand uncertainties can be addressed for microgrid resource planning. In addition, the index LOU_D enables system operators to understand various levels of uncertainty in the power grid.

VII. Acknowledgment

We acknowledge the suppot of National Science Foundation (award #1537565) for sponsoring this research.

References

[1] L. Funicello-Paul. *Global Revenue for Fixed Cost Microgrid O&M is Expected to Exceed $4 Billion in 2026*. NavigantResearch, 2017.

[2] S.A. Silling. *Reformulation of elasticity theory for discontinuities and long-range forces*. Journal of the Mechanics and Physics of Solids, 48 (2000), pp. 175-209.

[3] R.B. Lehoucq and S.A. Silling. *Peridynamic theory of solid mechanics*. Advances in Applied Mechanics, 44 (2010), pp. 73-166. we

[4] R. Haberman, *Applied Partial Differential Equations with Fourier Series and Boundary Value Problems*, 5th ed. (Pearson Education, Upper Saddle River NJ, 2013), pp. 137-139, 143.

[5] V. Guruswami and D. Zuckerman, "Robust Fourier and Polynomial Curve Fitting," *2016 IEEE 57th Annual Symposium on Foundations of Computer Science (FOCS)*, New Brunswick, NJ, 2016, pp. 751-759.

[6] M. Novosadov and P. Rajmic, "Piecewise-polynomial curve fitting using group sparsity," *2016 8th International Congress on Ultra Modern Telecommunications and Control Systems and Workshops (ICUMT)*, Lisbon, Portugal, 2016, pp. 320-325.

[7] L. Snyder and Z. Shen. *Supply and Demand Uncertainty in Multi-Echelon Supply Chains* Submitted for publication, Lehigh University 15 (2006).